




Article

Synchrotron Diffraction Study of the Crystal Structure of $\text{Ca}(\text{UO}_2)_6(\text{SO}_4)_2\text{O}_2(\text{OH})_6 \cdot 12\text{H}_2\text{O}$, a Natural Phase Related to Uranopilite

Sergey V. Krivovichev ^{1,2,*}, Nicolas Meisser ³, Joel Brugger ⁴, Dmitry V. Chernyshov ^{5,6}
and Vladislav V. Gurzhiy ²

¹ Nanomaterials Research Centre, Kola Science Centre, Russian Academy of Sciences, Fersmana 14, 184209 Apatity, Russia

² Department of Crystallography, Institute of Earth Sciences, St. Petersburg State University, University Emb. 7/9, 199034 St. Petersburg, Russia; vladislav.gurzhiy@spbu.ru

³ Musée cantonal de géologie, University of Lausanne, Anthropole, 1015 Lausanne, Switzerland; Nicolas.Meisser@unil.ch

⁴ School of Earth, Atmosphere and the Environment, Monash University, Clayton, Vic 3168, Australia; joel.brugger@monash.edu

⁵ Swiss-Norwegian Beamline, European Synchrotron Light Source, 38043 Grenoble CEDEX 9, France; dmitry.chernyshov@esrf.fr

⁶ Peter the Great St. Petersburg Polytechnic University, Polytekhnicheskaya 29, 195251 St. Petersburg, Russia

* Correspondence: s.krivovichev@spbu.ru; Tel.: +7-81555-7-53-50

Received: 27 October 2018; Accepted: 1 December 2018; Published: 4 December 2018



Abstract: The crystal structure of a novel natural uranyl sulfate, $\text{Ca}(\text{UO}_2)_6(\text{SO}_4)_2\text{O}_2(\text{OH})_6 \cdot 12\text{H}_2\text{O}$ (CaUS), has been determined using data collected under ambient conditions at the Swiss–Norwegian beamline BM01 of the European Synchrotron Research Facility (ESRF). The compound is monoclinic, $P2_1/c$, $a = 11.931(2)$, $b = 14.246(6)$, $c = 20.873(4)$ Å, $\beta = 102.768(15)$, $V = 3460.1(18)$ Å³, and $R_1 = 0.172$ for 3805 unique observed reflections. The crystal structure contains six symmetrically independent U^{6+} atoms forming (UO_7) pentagonal bipyramids that share O···O edges to form hexamers oriented parallel to the (010) plane and extended along [1–20]. The hexamers are linked via (SO_4) groups to form $[(\text{UO}_2)_6(\text{SO}_4)_2\text{O}_2(\text{OH})_6(\text{H}_2\text{O})_4]^{2-}$ chains running along the c -axis. The adjacent chains are arranged into sheets parallel to (010). The Ca^{2+} ions are coordinated by seven O atoms, and are located in between the sheets, providing their linkage into a three-dimensional structure. The crystal structure of CaUS is closely related to that of uranopilite, $(\text{UO}_2)_6(\text{SO}_4)\text{O}_2(\text{OH})_6 \cdot 14\text{H}_2\text{O}$, which is also based upon uranyl sulfate chains consisting of hexameric units formed by the polymerization of six (UO_7) pentagonal bipyramids. However, in uranopilite, each (SO_4) tetrahedron shares its four O atoms with (UO_7) bipyramids, whereas in CaUS, each sulfate group is linked to three uranyl ions only, and has one O atom (O16) linked to the Ca^{2+} cation. The chains are also different in the U:S ratio, which is equal to 6:1 for uranopilite and 3:1 for CaUS. The information-based structural complexity parameters for CaUS were calculated taking into account H atoms show that the crystal structure of this phase should be described as very complex, possessing 6.304 bits/atom and 1991.995 bits/cell. The high structural complexity of CaUS can be explained by the high topological complexity of the uranyl sulfate chain based upon uranyl hydroxo/oxo hexamers and the high hydration character of the phase.

Keywords: uranium; crystal structure; sulfate; minerals; uranopilite; synchrotron radiation; structural complexity

1. Introduction

It would not be an exaggeration to say that, within the last few years, uranium mineralogy and crystal chemistry has witnessed a true renaissance due to the discoveries of exceptional suites of new uranium minerals in Jáchymov, Czech Republic [1–6] and San Juan County, Utah, USA [7–19]. The diversity of new natural uranyl sulfates is of particular interest [1–5,7–15,17,18,20,21], since most of them do not have direct synthetic analogues, and are therefore new to the synthetic inorganic chemistry as well. Most of the new uranium sulfates are the products of secondary low-temperature hydrothermal processes, which are often associated with the crystallization of very complex mineral species such as ewingite, $\text{Mg}_8\text{Ca}_8(\text{UO}_2)_{24}(\text{CO}_3)_{30}\text{O}_4(\text{OH})_{12}(\text{H}_2\text{O})_{138}$, which is the most structurally complex mineral known today [6]. The structural architectures of novel natural uranyl sulfates show many similarities to synthetic uranyl sulfates, chromates, molybdates, and selenates, as reviewed by Krivovichev and Burns [22] and Krivovichev [23]. In most of them, uranyl ions are interlinked via tetrahedral TO_4 groups ($\text{T} = \text{S}, \text{Cr}, \text{Se}, \text{Mo}$) into finite clusters, chains, or layers, in which the interaction between adjacent uranyl groups is mediated by the hexavalent T^{6+} cations. For this group of minerals and synthetic compounds, the U:T ratio is usually smaller than one, with the ratio of 1:2 = 0.5 probably being the most common. However, there exists a group of uranyl sulfate mineral structures with an U:S ratio larger than one (e.g., 2:1 for the minerals of the zippeite group [1,5,17,24–28]) or equal to one (e.g., in adolpateraite, $\text{K}(\text{UO}_2)(\text{SO}_4)(\text{OH})(\text{H}_2\text{O})$ [2], and johannite, $\text{Cu}(\text{UO}_2)_2(\text{SO}_4)_2(\text{OH})_2 \cdot 8\text{H}_2\text{O}$ [29]). In these structures, uranyl ions are linked via common O^{2-} or $(\text{OH})^-$ anions, thus creating uranyl oxo/hydroxo substructures consisting of polymerized UO_n coordination polyhedra ($n = 5$ or 6). For instance, in the crystal structures of zippeite-group minerals, (UO_7) pentagonal bipyramids share edges to form infinite chains linked into $[(\text{UO}_2)_2(\text{SO}_4)\phi_2]$ sheets ($\phi = \text{O}^{2-}, (\text{OH})^-$) via (SO_4) tetrahedra [25]. The highest U:S ratios known so far are 8:1, which has been reported for jáchymovite, $(\text{UO}_2)_8(\text{SO}_4)(\text{OH})_{14} \cdot 13\text{H}_2\text{O}$ [30], and 6:1, which has been reported for both uranopilite, $(\text{UO}_2)_6(\text{SO}_4)\text{O}_2(\text{OH})_6 \cdot 14\text{H}_2\text{O}$, and metauranopilite, $(\text{UO}_2)_6(\text{SO}_4)(\text{OH})_{10} \cdot 5\text{H}_2\text{O}$ (?) [31]. Burns reported that the crystal structure of uranopilite is based upon chains consisting of hexamers of edge-sharing (UO_7) pentagonal bipyramids linked by (SO_4) tetrahedra (the crystal structures of jáchymovite and metauranopilite are still unknown) [32].

Herein, we report on the synchrotron radiation study of $\text{Ca}(\text{UO}_2)_6(\text{SO}_4)_2\text{O}_2(\text{OH})_6 \cdot 12\text{H}_2\text{O}$ (CaUS), which is a new natural phase with a chemical composition and crystal structure that has no analogues among the known minerals and synthetic compounds. From the viewpoint of chemistry, CaUS is closely related to rabejacite, $\text{Ca}(\text{UO}_2)_2(\text{SO}_4)\text{O}_2 \cdot 4\text{H}_2\text{O}$, which is the secondary uranyl sulfate of the zippeite group [28,32].

2. Materials and Methods

2.1. Occurrence

The new oxyhydrated calcium uranyl sulfate mineral phase (“CaUS”) was collected in December 1985 by one of us (NM) in underground prospecting and mining workings of La Creusaz U-deposit near Les Marécottes, Valais, Switzerland. In 1986, CaUS was analyzed using powder X-ray diffraction (XRD), which indicated that it has no analogues among natural and synthetic phases [33].

Since the end of the underground workings in 1981, outcropping veins and stockpiled high-grade U-ore (average of three analyses: U 0.8 wt.%, S 0.5 wt.%, Bi 0.1 wt.%, Pb 870 ppm, Cu 680 ppm, Zn 300 ppm, and As 200 ppm) have been exposed to acid mine drainage water and atmospheric oxygen in the abandoned galleries. The oxidation of the sulfides (mainly pyrite and chalcopyrite) under the presence of strong bacterial activity resulted in the production of acidic ($\text{pH} = 3.1$), sulfate-rich waters. These waters reacted with uraninite, clinocllore, illite, calcite, and siderite and, after in situ natural evaporation, formed a rich assemblage of secondary uranyl sulfates minerals, including (by decreasing abundance): schröckingerite, uranopilite, marécottite, magnesiozippeite, johannite, pseudojohannite, rabejacite, zippeite, natrozippeite, coconinoite, jáchymovite, and the CaUS phase described here.

More than 30 other U-bearing minerals have been described in the La Creusaz mine, and this deposit is the type locality of three of them: marécottite, $\text{Mg}_3(\text{UO}_2)_8(\text{SO}_4)_4\text{O}_6(\text{OH})_2 \cdot 28\text{H}_2\text{O}$ [26], pseudojohannite, $\text{Cu}_3(\text{OH})_2[(\text{UO}_2)_4(\text{SO}_4)_2] \cdot 12\text{H}_2\text{O}$ [34], and françoisite-(Ce), $(\text{Ce}, \text{Nd}, \text{Ca})(\text{UO}_2)_3(\text{PO}_4)_2\text{O}(\text{OH}) \cdot 6\text{H}_2\text{O}$ [35].

The CaUS phase appears as lemon yellow, hemispheric efflorescent aggregates on an ore matrix that are up to four mm, and consists of tiny platy prismatic crystals with typical monoclinic forms up to 0.1 mm (Figure 1). The mineral is not fluorescent. Other supergene mineral species directly associated with CaUS on the same sample are: uranopilite, rabejacite, magnesiozippeite, and gypsum.

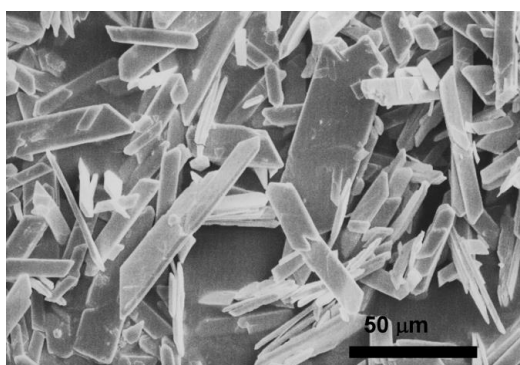


Figure 1. SEM-BSE (scanning-electron microscopic back-scattered electron) image of $\text{Ca}(\text{UO}_2)_6(\text{SO}_4)_2\text{O}_2(\text{OH})_6 \cdot 12\text{H}_2\text{O}$ (CaUS) mineral phase. Note the typical monoclinic shapes of the crystals.

Despite intense field investigations conducted from 1988 to 2015, to date, only one specimen of the mineral is known, which was collected only four years after the end of the mining works, and deposited in Musée Cantonal de Géologie of Lausanne (Switzerland) under research collection number: XRD-NM-0005. The data on this mineral presently known do not allow its full description as a new mineral species, until more material is found.

2.2. Chemical Composition

Semi-quantitative chemical analyses were carried out by means of scanning electron microscope CamScan MV2300 coupled with an energy-dispersive spectrometer Inca x-sight Oxford Instruments (Institut des sciences de la Terre, Faculté des géosciences et de l'environnement, University of Lausanne, Lausanne, Switzerland). Five analyses of 100-s each were conducted using a large focused beam scanned over a surface of about $100 \mu\text{m}^2$, an accelerating voltage of 20 kV, a sample current of $40 \mu\text{A}$, and a vacuum of $1.5 \cdot 10^{-5}$ Pa. The following X-ray lines and analytical standards were used: U $M\alpha$ - UO_2 , Ca $K\alpha$ - CaSO_4 , and S $K\alpha$ - CaSO_4 . Despite various analytical problems due to intense dehydration under electron beam, only Ca, U, S, Ca, and O were detected with the average ratio Ca:U:S~1:5.6:2.2.

2.3. Synchrotron Single-Crystal X-Ray Diffraction Study

Synchrotron diffraction experiment was performed under ambient conditions at the Swiss–Norwegian beamline BM01 of the European Synchrotron Research Facility (ESRF) with an imaging plate area detector (Mar345; 2300×2300 pixels) that had a crystal-to-detector distance of 160 mm. A yellow needle-like crystal of CaUS was mounted on a tapered glass fiber and centered using a high-magnification CCD (charge-coupled device) camera. Diffraction data were measured using monochromatized radiation ($\lambda = 0.80000 \text{ \AA}$) in an oscillation mode by rotating the crystal in φ by 2° two minutes per frame; 100 frames were measured. The intensities were integrated and merged with the program CrysAlis. Lorentz and polarization corrections were applied; absorption effects were corrected using SADABS ($R_{\text{int}} = 0.144$). The structure was solved using the SHELXS program [36]. The agreement factor for the final model was $R_1 = 0.173$ for 3805 unique observed reflections with $|F_o| \geq 4\sigma_F$. The crystallographic information and refinement parameters are given

in Table 1. The poor quality of the diffraction data (the highest resolution = 1.09 Å) did not allow the refinement of positions of oxygen atoms in an anisotropic approximation. In addition, soft restraints were imposed upon the uranyl U–O and some S–O distances in order to keep the bond lengths of the uranyl ions within the crystal chemically realistic values. No positions of H atoms could be determined. Atom coordinates, isotropic parameters, and bond-valence sums (calculated using bond-valence parameters for the U–O bonds taken from Burns et al. [37] and for other bonds from Gagné and Hawthorne [38]) are given in Table 2. Table 3 provides the anisotropic displacement parameters for the U, Ca, and S atoms. Selected bond lengths are given in Table 4. Supplementary crystallographic data have been deposited in the Inorganic Crystal Structure Database (CSD 1873912), and can be obtained from Fachinformationszentrum Karlsruhe via <https://www.ccdc.cam.ac.uk/structures/>.

Table 1. Crystal data and structure refinement for Ca(UO₂)₆(SO₄)₂O₂(OH)₆·12H₂O (CaUS).

Crystal System	Monoclinic
Space group	<i>P</i> 2 ₁ / <i>c</i>
<i>a</i> , Å	11.931(2)
<i>b</i> , Å	14.246(6)
<i>c</i> , Å	20.873(4)
β , °	102.768(15)
<i>V</i> , Å ³	3460.1(18)
<i>Z</i>	4
ρ_{calc} , g/cm ³	4.170
μ , mm ^{−1}	16.244
Crystal dimensions, μm	2 × 3 × 12
λ , Å	0.800000
2 θ range, deg.	4.92–43.22
Index ranges	−12 ≤ <i>h</i> ≤ 12, −14 ≤ <i>k</i> ≤ 14, −21 ≤ <i>l</i> ≤ 21
Reflections collected	12545
Independent reflections	3805 [<i>R</i> _{int} = 0.144]
Data/restraints/parameters	3805/12/243
GOF	1.049
Final <i>R</i> indexes [<i>I</i> ≥ 2 σ (<i>I</i>)]	<i>R</i> ₁ = 0.173, <i>wR</i> ₂ = 0.380, <i>R</i> _{free} = 0.192
Final <i>R</i> indexes [all data]	<i>R</i> ₁ = 0.179, <i>wR</i> ₂ = 0.386, <i>R</i> _{free} = 0.201

Table 2. Atomic coordinates, isotropic displacement parameters (Å²), and bond valence sums (BVS, in valence units (v.u.)) for CaUS.

Atom	<i>x</i>	<i>y</i>	<i>z</i>	<i>U</i> _{eq}	BVS
U1	0.7442(2)	0.3460(2)	0.74651(13)	0.0448(9)	6.36
U2	1.0278(2)	0.2113(2)	0.59440(14)	0.0471(9)	6.29
U3	0.4738(2)	0.2605(2)	0.79912(14)	0.0472(9)	6.23
U4	0.0512(2)	0.3457(2)	0.91572(13)	0.0447(9)	6.28
U5	0.7282(2)	0.3397(2)	0.92816(13)	0.0450(9)	6.26
U6	0.2940(2)	0.2244(2)	1.03222(14)	0.0476(9)	6.02
S1	1.0408(16)	0.3614(15)	0.7353(8)	0.045(5)	5.85
S2	0.7350(15)	0.2058(14)	0.6043(9)	0.043(5)	6.09
Ca	0.8799(16)	0.0915(14)	0.8342(9)	0.068(5)	1.77
O1	0.694(4)	0.458(2)	0.723(2)	0.043(12)	1.82
O2	0.806(4)	0.239(2)	0.774(2)	0.032(10)	2.08
O3	0.978(6)	0.323(3)	0.573(4)	0.09(2)	1.85
O4	1.081(5)	0.105(3)	0.627(3)	0.067(16)	1.85
O5	0.397(4)	0.364(3)	0.781(3)	0.054(14)	1.85
O6	0.540(4)	0.152(2)	0.819(2)	0.043(12)	1.82
O7	0.086(4)	0.462(2)	0.935(2)	0.042(12)	1.85
O8	0.003(5)	0.235(2)	0.889(3)	0.065(16)	2.02
O9	0.698(6)	0.455(2)	0.943(3)	0.080(19)	1.85
O10	0.768(5)	0.225(2)	0.918(3)	0.070(17)	1.89
O11	0.226(4)	0.118(2)	1.001(2)	0.053(13)	1.71
O12	0.372(4)	0.323(3)	1.064(3)	0.053(14)	1.82
O13	1.088(5)	0.360(4)	0.806(3)	0.060(15)	2.02
O14	1.033(4)	0.268(3)	0.704(2)	0.045(12)	1.97
O15	0.920(4)	0.401(4)	0.721(3)	0.052(13)	1.85

Table 2. Cont.

Atom	x	y	z	U_{eq}	BVS
O16	0.893(5)	−0.073(4)	0.798(3)	0.071(17)	1.71
O17	0.845(4)	0.163(3)	0.623(2)	0.028(10)	2.14
O18	0.739(4)	0.296(3)	0.639(2)	0.042(12)	2.07
O19	0.709(4)	0.224(3)	0.533(2)	0.042(12)	1.91
O20	0.654(5)	0.140(4)	0.626(4)	0.09(2)	1.43
O _H 21	−0.140(3)	0.401(3)	0.8570(19)	0.023(9)	1.19
O _H 22	0.558(3)	0.277(3)	0.705(2)	0.026(10)	0.98
O _H 23	0.247(4)	0.304(3)	0.920(2)	0.037(11)	0.88
O _H 24	1.204(5)	0.285(4)	0.622(3)	0.050(13)	1.14
O25	0.639(4)	0.351(3)	0.819(2)	0.042(12)	1.98
O _H 26	0.915(4)	0.130(3)	0.494(2)	0.040(11)	1.27
O27	1.126(6)	0.205(5)	0.513(3)	0.079(19)	2.20
O _H 28	0.531(5)	0.300(4)	0.910(3)	0.062(15)	1.10
O _W 29	0.460(4)	0.171(3)	0.995(3)	0.049(13)	0.49
O _W 30	0.311(8)	0.193(6)	0.842(5)	0.11(3)	0.42
O _W 31	0.341(5)	0.179(4)	0.712(3)	0.058(15)	0.48
O _W 32	0.424(4)	0.377(3)	0.620(3)	0.048(13)	0.36
O _W 33	0.730(6)	0.025(4)	0.884(3)	0.074(18)	0.27
O _W 34	0.724(5)	0.046(4)	0.745(3)	0.068(16)	0.29
O _W 35	1.035(8)	0.096(7)	0.780(5)	0.13(3)	0.32
O _W 36	1.014(8)	0.024(6)	0.932(5)	0.12(3)	0.24
O _W 37	0.396(5)	0.461(4)	0.938(3)	0.064(16)	-
O _W 38	0.448(6)	0.034(5)	0.674(4)	0.09(2)	-
O _W 39	0.724(6)	0.420(5)	0.511(4)	0.09(2)	-
O _W 40	0.577(4)	0.510(3)	0.581(2)	0.046(12)	-

Table 3. Anisotropic displacement atom parameters for CaUS (Å²).

Atom	U^{11}	U^{22}	U^{33}	U^{23}	U^{13}	U^{12}
U1	0.0358(17)	0.076(2)	0.0297(16)	−0.0003(13)	0.0238(14)	0.0023(13)
U2	0.0338(17)	0.081(2)	0.0326(17)	−0.0028(13)	0.0199(14)	−0.0001(14)
U3	0.0351(17)	0.081(2)	0.0312(16)	−0.0053(14)	0.0190(14)	−0.0001(14)
U4	0.0339(17)	0.078(2)	0.0269(16)	−0.0010(13)	0.0168(13)	0.0020(13)
U5	0.0355(17)	0.077(2)	0.0281(16)	−0.0003(13)	0.0198(13)	−0.0009(13)
U6	0.0350(18)	0.079(2)	0.0356(17)	0.0000(13)	0.0211(14)	0.0025(14)
S1	0.026(11)	0.067(15)	0.036(8)	−0.006(8)	0.014(8)	−0.005(10)
S2	0.026(10)	0.068(13)	0.037(11)	−0.010(9)	0.013(9)	−0.003(8)
Ca	0.061(12)	0.082(14)	0.065(12)	−0.007(10)	0.025(10)	−0.027(10)

Table 4. Selected bond lengths (Å) in the crystal structure of CaUS.

Bond	Bond Length	Bond	Bond Length	Bond	Bond Length
U1–O2	1.73(2)	U3–O5	1.73(3)	U5–O10	1.72(3)
U1–O1	1.74(3)	U3–O6	1.74(3)	U5–O9	1.73(3)
U1–O25	2.18(5)	U3–O25	2.31(5)	U5–O25	2.29(5)
U1–O18	2.34(5)	U3–O _H 28	2.33(6)	U5–O _H 28	2.37(6)
U1–O _H 22	2.41(4)	U3–O _H 22	2.41(4)	U5–O _H 26	2.39(5)
U1–O15	2.41(5)	U3–O _W 31	2.42(6)	U5–O19	2.42(5)
U1–O _H 21	2.54(4)	U3–O _W 30	2.49(9)	U5–O _H 21	2.54(4)
U2–O3	1.73(3)	U4–O7	1.73(3)	U6–O12	1.74(3)
U2–O4	1.73(3)	U4–O8	1.73(3)	U6–O11	1.77(3)
U2–O27	2.26(7)	U4–O27	2.16(7)	U6–O27	2.20(7)
U2–O _H 24	2.30(5)	U4–O _H 23	2.39(5)	U6–O _H 24	2.37(5)
U2–O14	2.41(5)	U4–O13	2.43(6)	U6–O _W 29	2.40(5)
U2–O17	2.48(4)	U4–O _H 21	2.47(4)	U6–O _H 23	2.55(5)
U2–O _H 26	2.51(5)	U4–O _H 26	2.57(5)	U6–O _W 32	2.56(5)
Ca–O _W 35	2.37(10)	S1–O13	1.46(6)	S2–O17	1.42(5)
Ca–O _W 34	2.41(6)	S1–O14	1.48(5)	S2–O18	1.47(5)
Ca–O _W 33	2.44(7)	S1–O16	1.48(6)	S2–O19	1.49(5)
Ca–O16	2.49(6)	S1–O15	1.51(6)	S2–O20	1.49(2)
Ca–O _W 36	2.49(10)	<S1–O>	1.483	<S2–O>	1.468
Ca–O2	2.51(3)				
Ca–O8	2.62(4)				
<Ca–O>	2.476				

3. Results

The crystal structure of CaUS (Figure 2) contains six symmetrically independent U sites, each forming two short (1.72–1.77 Å) U=O bonds, which results in the formation of linear uranyl cations, $(\text{UO}_2)^{2+}$. In equatorial planes, each uranyl ion is coordinated by five O atoms that belong either to sulfate groups, hydroxyl ions, or H_2O molecules. The (UO_7) pentagonal bipyramids share O···O edges to form hexamers that are oriented parallel to the (010) plane and extended along [1–20] (Figure 3). The hexamers are linked via (SO_4) groups to form $[(\text{UO}_2)_6(\text{SO}_4)_2\text{O}_2(\text{OH})_6(\text{H}_2\text{O})_4]^{2-}$ chains running along the *c*-axis. The adjacent chains are arranged into sheets parallel to (010) (Figure 3). The Ca^{2+} ions are coordinated by seven O atoms, and are located in between the sheets, providing their linkage into a three-dimensional structure (Figure 4). The average $\langle\text{S–O}\rangle$ bond length in sulfate tetrahedra is equal to 1.483 and 1.468 Å for S1 and S2, respectively, which is in good agreement with the grand average value of 1.473 Å calculated for sulfates by Hawthorne et al. [39].

The crystal structure of CaUS contains three different types of H_2O groups. The $\text{H}_2\text{O}_{29}\text{--H}_2\text{O}_{32}$ groups (corresponding to the $\text{O}_{\text{W}29}\text{--O}_{\text{W}32}$) are bonded to U^{6+} cations, and therefore are the parts of the basic structural unit, i.e., the uranyl sulfate chains. The $\text{H}_2\text{O}_{33}\text{--H}_2\text{O}_{36}$ groups are bonded to Ca^{2+} cations, and are located in between the chains, whereas the $\text{H}_2\text{O}_{37}\text{--H}_2\text{O}_{40}$ groups are held in the structure by the system of hydrogen bonds. Since the positions of the H atoms are unknown, no attempt was made to outline the possible hydrogen bonding system, since each potential donor/acceptor O atom has too many adjacent O atoms at the distances appropriate for the formation of a hydrogen bond.

The results of the bond valence analysis are given in Table 2. The bond valence sums (BVSs) for U atoms are in the range of 6.02–6.36 v.u., which is acceptable, taking into account that the U=O bond lengths within the uranyl ions were constrained. The BVSs for the S1, S2, and Ca sites are 5.85 v.u., 6.09 v.u., and 1.77 v.u., respectively. The BVSs for the O atoms assigned to hydroxyl ions range from 0.88 v.u. to 1.27 v.u., those for the H_2O molecules vary from 0.00 (for the groups not bonded to U or Ca) to 0.49 v.u. The BVSs for the O atoms are in the range of 1.82–2.20 v.u., except for the O20 site, for which the BVS is equal to 1.43 v.u. However, the O20 atom is bonded to the S^{6+} cation only, and has two adjacent H_2O groups and one OH group at distances ranging from 2.74 Å to 2.97 Å. Therefore, it is most probable that this atom is involved in three moderate hydrogen bonds, which saturate its bond valence requirements.

According to the crystal structure refinement, the crystal chemical formula of CaUS can be written as $\text{Ca}[(\text{UO}_2)_6(\text{SO}_4)_2\text{O}_2(\text{OH})_6(\text{H}_2\text{O})_4]\cdot(\text{H}_2\text{O})_8$ (with the chemical formula of the uranyl sulfate chain given in square brackets).

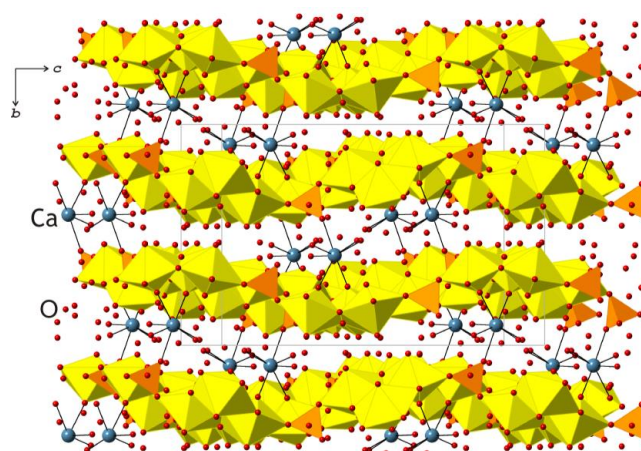


Figure 2. The crystal structure of CaUS projected onto the (100) plane. Legend: U and S polyhedra are shown in yellow and orange colors, respectively; Ca and O atoms are shown as dark blue and red spheres, respectively.

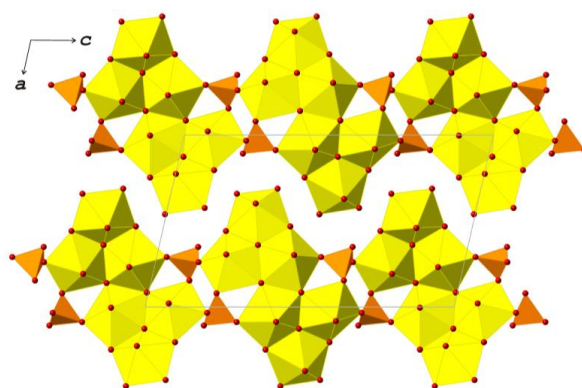


Figure 3. The layer of the $[(\text{UO}_2)_6(\text{SO}_4)_2\text{O}_2(\text{OH})_6(\text{H}_2\text{O})_4]^{2-}$ chains in the crystal structure of CaUS. Legend is as in Figure 1.

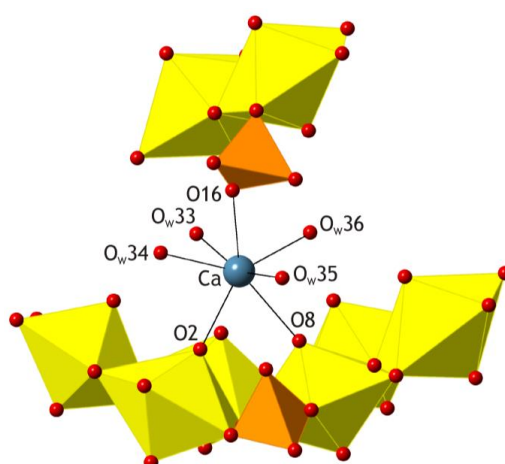


Figure 4. Coordination of Ca^{2+} cation in the crystal structure of CaUS. Legend is as in Figure 2.

4. Discussion

The crystal structure of CaUS is closely related to that of uranopilite, $(\text{UO}_2)_6(\text{SO}_4)\text{O}_2(\text{OH})_6 \cdot 14\text{H}_2\text{O}$ [32], which is also based upon uranyl sulfate chains consisting of hexameric units formed by the polymerization of six (UO_7) pentagonal bipyramids (Figure 5b). However, in uranopilite, each (SO_4) tetrahedron shares its four O atoms with (UO_7) bipyramids (as also observed in zippeite-group minerals [1,5,17,24–28]), whereas, in CaUS, each sulfate group is linked to three uranyl ions only, and has one O atom (O16) linked to the Ca^{2+} cation. The chains are also different in the U:S ratio, which is equal to 6:1 for uranopilite and 3:1 for CaUS.

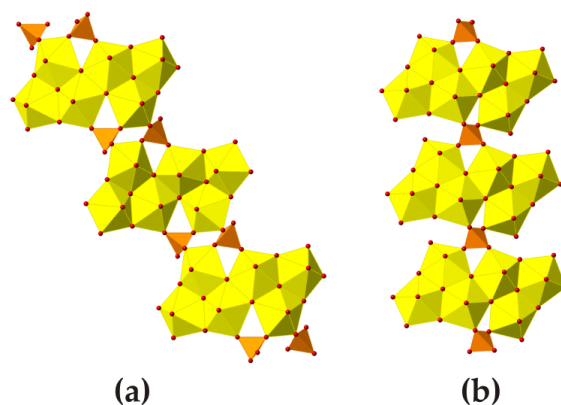


Figure 5. The uranyl sulfate chains in the crystal structures of CaUS (a) and uranopilite (b).

The information-based complexity parameters [40,41] for CaUS are given in Table 5. Calculations have been performed in several steps. At first, the structural complexity of the uranyl sulfate chain has been analyzed, taking into account its real rod symmetry group (RG, Figure 6a). Secondly, the topological complexity of the chain (according to the maximal RG) has been calculated (Figure 6b). Then, complexity parameters for the uranyl sulfate substructure (i.e., two chains per unit cell) and for the whole structure have been calculated using *ToposPro* package [42], and are given in Table 5 for comparison. It should be taken into account that to process the complexity measures, the positions of all of the H atoms have been assigned manually in calculated positions considering the distribution of the H-bonding system. Complexity calculations show that the crystal structure of CaUS should be described as very complex, possessing 6.304 bits/atom and 1991.995 bits/cell. For comparison, the crystal structure of uranopilite should be considered as complex (6.304 bits/atom and 995.997 bits/cell), while the most frequent values of structural complexity of the natural uranyl sulfates (including H-atoms) are between 500–600 bits/cell [43]. The high structural complexity of CaUS can be explained by the high topological complexity of the uranyl sulfate chain based upon uranyl hydroxo/oxo hexamers and the high hydration character of the phase. Both features are typical for low-temperature mineral phases that form in the oxidation zones of mineral deposits [37,44–46].

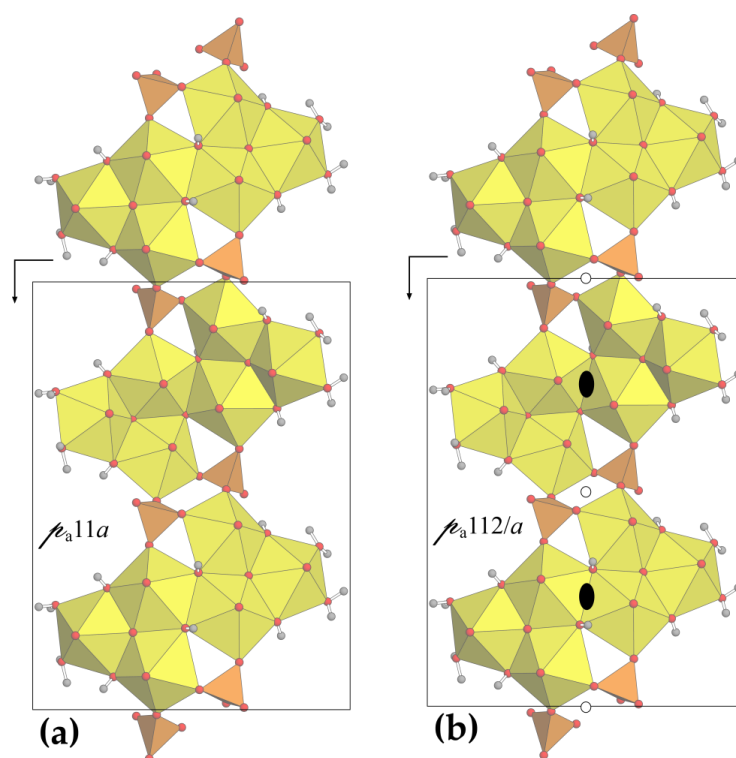


Figure 6. Real (a) and maximal (b) rod symmetry groups of the uranyl sulfate chains observed in CaUS. Rod group is an affine subperiodic three-dimensional group type with one-dimensional translation that are classified analogously to the space groups. Subindex “a” in a rod group symbol indicates the $(-cba)$ setting with the translation along the a direction. The symmetry operations for (a) are: $1/2 + x, y, -z$; and for (b) are: $1/2 - x, -y, z$; $1/2 + x, y, -z$; and $-x, -y, -z$.

Table 5. Information-based topological and structural complexity parameters for CaUS.

	ν (atoms)	I_G (bits/atom)	$I_{G, total}$ (bits/cell)	Contribution to $I_{G, total}$ (%)
Topological complexity of the US chain	108	4.755	513.528	25.78
Structural complexity of the US chain	108	5.755	621.528	31.20
Structural complexity of the US substructure (two chains per cell)	216	5.755	1243.056	62.40
Total structural complexity for CaUS	316	6.304	1991.995	100

Author Contributions: Conceptualization, N.M., J.B., V.V.G. and S.V.K.; Methodology, S.V.K., N.M. and D.Y.C.; Investigation, S.V.K., N.M. and D.Y.C.; Writing-Original Draft Preparation, S.V.K., N.M., V.V.G.; Writing-Review and Editing, S.V.K., N.M., and V.V.G.; Visualization, S.V.K., N.M., V.V.G.

Funding: This research was funded by the Russian Science Foundation (grant 18-17-00018 to V.V.G.). Portions of this research were funded by the European Synchrotron Research Facility, Swiss-Norwegian Beam Line.

Acknowledgments: We are grateful to reviewers for useful comments. We are grateful to Pierre Vonlanthen (SEM laboratory, Institut des sciences de la Terre, University of Lausanne) for the help with the SEM.

Conflicts of Interest: The authors declare no conflict of interest.

References

- Plášil, J.; Dušek, M.; Novák, M.; Čejka, J.; Císařová, I.; Škoda, R. Sejkoraite-(Y), a new member of the zippeite group containing trivalent cations from Jáchymov (St. Joachimsthal), Czech Republic: Description and crystal structure refinement. *Am. Mineral.* **2011**, *96*, 983–991. [[CrossRef](#)]
- Plášil, J.; Hloušek, J.; Veselovský, F.; Fejfarová, K.; Dušek, M.; Škoda, R.; Novák, M.; Čejka, J.; Sejkora, J.; Ondruš, P. Adolfpateraite, $K(UO_2)(SO_4)(OH)(H_2O)$, a new uranyl sulphate mineral from Jáchymov, Czech Republic. *Am. Mineral.* **2012**, *97*, 447–454. [[CrossRef](#)]
- Plášil, J.; Veselovský, F.; Hloušek, J.; Šák, M.; Sejkora, J.; Čejka, J.; Škacha, P.; Kasatkin, A.V. Mathesiusite, $K_5(UO_2)_4(SO_4)_4(VO_5)(H_2O)_4$, a new uranyl vanadate-sulfate from Jáchymov, Czech Republic. *Am. Mineral.* **2014**, *99*, 625–632. [[CrossRef](#)]
- Plášil, J.; Hloušek, J.; Kasatkin, A.V.; Škoda, R.; Novák, M.; Čejka, J. Geschieberite, $K_2(UO_2)(SO_4)_2(H_2O)_2$, a new uranyl sulfate mineral from Jáchymov. *Mineral. Mag.* **2015**, *79*, 205–216. [[CrossRef](#)]
- Plášil, J.; Škacha, P.; Sejkora, J.; Kampf, A.R.; Škoda, R.; Čejka, J.; Hloušek, J.; Kasatkin, A.V.; Pavlíček, R.; Babka, K. Plavnoite, a new K-Mn member of the zippeite group from Jáchymov, Czech Republic. *Eur. J. Mineral.* **2017**, *29*, 117–128. [[CrossRef](#)]
- Olds, T.A.; Plášil, J.; Kampf, A.R.; Simonetti, A.; Sadergaski, L.R.; Chen, Y.S.; Burns, P.C. Ewingite: Earth's most complex mineral. *Geology* **2017**, *45*, 1007–1010. [[CrossRef](#)]
- Plášil, J.; Kampf, A.R.; Kasatkin, A.V.; Marty, J.; Škoda, R.; Silva, S.; Čejka, K. Meisserite, $Na_5(UO_2)(SO_4)_3(SO_3OH)(H_2O)$, a new uranyl sulfate mineral from the Blue Lizard mine, San Juan County, Utah, USA. *Mineral. Mag.* **2013**, *77*, 2975–2988. [[CrossRef](#)]
- Kampf, A.R.; Plášil, J.; Kasatkin, A.V.; Marty, J. Belakovskiite, $Na_7(UO_2)(SO_4)_4(SO_3OH)(H_2O)_3$, a new uranyl sulfate mineral from the Blue Lizard mine, San Juan County, Utah, USA. *Mineral. Mag.* **2014**, *78*, 639–649. [[CrossRef](#)]
- Plášil, J.; Kampf, A.R.; Kasatkin, A.V.; Marty, J. Bluelizardite, $Na_7(UO_2)(SO_4)_4Cl(H_2O)_2$, a new uranyl sulfate mineral from the Blue Lizard mine, San Juan County, Utah, USA. *J. Geosci.* **2014**, *59*, 145–158. [[CrossRef](#)]
- Kampf, A.R.; Plášil, J.; Kasatkin, A.V.; Marty, J. Bobcookite, $NaAl(UO_2)_2(SO_4)_4 \cdot 18H_2O$ and wetherillite, $Na_2Mg(UO_2)_2(SO_4)_4 \cdot 18H_2O$, two new uranyl sulfate minerals from the Blue Lizard mine, San Juan County, Utah, USA. *Mineral. Mag.* **2015**, *79*, 695–714. [[CrossRef](#)]
- Kampf, A.R.; Plášil, J.; Kasatkin, A.V.; Marty, J.; Čejka, J. Fermiite, $Na_4(UO_2)(SO_4)_3 \cdot 3H_2O$, and oppeneimerite, $Na_2(UO_2)(SO_4)_2 \cdot 3H_2O$, two new uranyl sulfate minerals from the Blue Lizard mine, San Juan County, Utah, USA. *Mineral. Mag.* **2015**, *79*, 1123–1142. [[CrossRef](#)]
- Kampf, A.R.; Kasatkin, A.V.; Čejka, J.; Marty, J. Plášilite, $Na(UO_2)(SO_4)(OH) \cdot 2H_2O$, a new uranyl sulfate mineral from the Blue Lizard mine, San Juan County, Utah, USA. *J. Geosci.* **2015**, *60*, 1–10. [[CrossRef](#)]

13. Kampf, A.R.; Plášil, J.; Čejka, J.; Marty, J.; Škoda, R.; Lapčák, L. Alwilkinsite-(Y), a new rare-earth uranyl sulfate mineral from the Blue Lizard mine, San Juan County, Utah, USA. *Mineral. Mag.* **2017**, *81*, 895–907. [[CrossRef](#)]
14. Kampf, A.R.; Plášil, J.; Kasatkin, A.V.; Marty, J.; Čejka, J. Klaprothite, péligotite and ottohahnite, three new minerals with bidentate $\text{UO}_7\text{-SO}_4$ linkages from the Blue Lizard mine, San Juan County, Utah, USA. *Mineral. Mag.* **2017**, *81*, 753–779. [[CrossRef](#)]
15. Kampf, A.R.; Plášil, J.; Kasatkin, A.V.; Marty, J.; Čejka, J.; Lapčák, L. Shumwayite, $[(\text{UO}_2)(\text{SO}_4)(\text{H}_2\text{O})_2]_2 \cdot \text{H}_2\text{O}$, a new uranyl sulfate mineral from Red Canyon, San Juan County, Utah, USA. *Mineral. Mag.* **2017**, *81*, 273–285. [[CrossRef](#)]
16. Olds, T.A.; Sadergaski, L.R.; Plášil, J.; Kampf, A.R.; Burns, P.C.; Steele, I.M.; Marty, J.; Carlson, S.M.; Mills, O.P. Leószilárdite, the first Na,Mg-containing uranyl carbonate from the Markey Mine, San Juan County, Utah, USA. *Mineral. Mag.* **2017**, *81*, 1039–1050. [[CrossRef](#)]
17. Kampf, A.R.; Plášil, J.; Olds, T.A.; Nash, B.P.; Marty, J. Ammoniozippeite, a new uranyl sulfate mineral from the Blue Lizard mine, San Juan County, Utah, and the Burro mine, San Miguel County, Colorado, USA. *Can. Mineral.* **2018**, *56*, 235–245. [[CrossRef](#)]
18. Kampf, A.R.; Plášil, J.; Nash, B.P.; Marty, J. Greenlizardite, $(\text{NH}_4)\text{Na}(\text{UO}_2)_2(\text{SO}_4)_2(\text{OH})_2 \cdot 4\text{H}_2\text{O}$, a new mineral with phosphuranylite-type uranyl sulfate sheets from Red Canyon, San Juan County, Utah, USA. *Mineral. Mag.* **2018**, *82*, 401–411. [[CrossRef](#)]
19. Olds, T.A.; Plášil, J.; Kampf, A.R.; Spano, T.; Haynes, P.; Carlson, S.M.; Burns, P.C.; Simonetti, A.; Mills, O.P. Leesite, $\text{K}(\text{H}_2\text{O})_2[(\text{UO}_2)_4\text{O}_2(\text{OH})_5] \cdot 3\text{H}_2\text{O}$, a new K-bearing schoepite-family mineral from the Jomac mine, San Juan County, Utah, U.S.A. *Am. Mineral.* **2018**, *103*, 143–150. [[CrossRef](#)]
20. Pekov, I.V.; Krivovichev, S.V.; Yapaskurt, V.O.; Chukanov, N.V.; Belakovskiy, D.I. Beshtauite, $(\text{NH}_4)_2(\text{UO}_2)(\text{SO}_4)_2 \cdot 2\text{H}_2\text{O}$, a new mineral from Mount Beshtau, Northern Caucasus, Russia. *Am. Mineral.* **2014**, *99*, 1783–1787. [[CrossRef](#)]
21. Plášil, J.; Kasatkin, A.V.; Škoda, R.; Novák, M.; Kallistová, A.; Dušek, M.; Skála, R.; Fejfarová, K.; Čejka, J.; Meisser, N.; et al. Leydetite, $\text{Fe}(\text{UO}_2)(\text{SO}_4)_2(\text{H}_2\text{O})_{11}$, a new uranyl sulfate mineral from Mas d’Alary, Lodève, France. *Mineral. Mag.* **2013**, *77*, 429–441. [[CrossRef](#)]
22. Krivovichev, S.V.; Burns, P.C. Actinide compounds containing hexavalent cations of the VI group elements (S, Se, Mo, Cr, W). In *Structural Chemistry of Inorganic Actinide Compounds*; Krivovichev, S.V., Burns, P.C., Tananaev, I.G., Eds.; Elsevier: Amsterdam, The Netherlands, 2007; pp. 95–182.
23. Krivovichev, S.V. Actinyl compounds with hexavalent elements (S, Cr, Se, Mo)—Structural diversity, nanoscale chemistry, and cellular automata modeling. *Eur. J. Inorg. Chem.* **2010**, *2010*, 2594–2603. [[CrossRef](#)]
24. Frondel, C.; Ito, J.; Honea, R.M.; Weeks, A.M. Mineralogy of the zippeite group. *Can. Mineral.* **1976**, *14*, 429–436.
25. Burns, P.C.; Deely, K.M.; Hayden, L.A. The crystal chemistry of the zippeite group. *Can. Mineral.* **2003**, *41*, 687–706. [[CrossRef](#)]
26. Brugger, J.; Burns, P.C.; Meisser, N. Contribution to the mineralogy of acid drainage of uranium minerals: Marcottite and the zippeite-group. *Am. Mineral.* **2003**, *88*, 676–685. [[CrossRef](#)]
27. Plášil, J.; Fejfarová, K.; Wallwork, K.S.; Dušek, M.; Škoda, R.; Sejkora, J.; Čejka, J.; Veselovský, F.; Hloušek, J.; Meisser, N.; et al. Crystal structure of pseudojohannite, with a revised formula, $\text{Cu}_3(\text{OH})_2[(\text{UO}_2)_4\text{O}_4(\text{SO}_4)_2](\text{H}_2\text{O})_{12}$. *Am. Mineral.* **2012**, *97*, 1796–1803. [[CrossRef](#)]
28. Plášil, J.; Dušek, M.; Čejka, J.; Sejkora, J. The crystal structure of rabejacite, the Ca^{2+} -dominant member of the zippeite group. *Mineral. Mag.* **2014**, *78*, 1249–1264. [[CrossRef](#)]
29. Mereiter, K. Die Kristallstruktur des Johannites, $\text{Cu}(\text{UO}_2)_2(\text{OH})_2(\text{SO}_4)_2 \cdot 8\text{H}_2\text{O}$. *Tscherm. Mineral. Petrogr. Mitt.* **1982**, *30*, 47–57. [[CrossRef](#)]
30. Čejka, J.; Sejkora, J.; Mrázek, Z.; Urbanec, Z.; Jarchovský, T. Jáchymovite, $(\text{UO}_2)_8(\text{SO}_4)(\text{OH})_{14} \cdot 13\text{H}_2\text{O}$, a new uranyl mineral from Jáchymov, the Krušné hory Mts., Czech Republic, and its comparison with uranopilite. *Neues Jahrb. Mineral. Abh.* **1996**, *170*, 155–170.
31. Frondel, C. Studies of uranium minerals (X): Uranopilite. *Am. Mineral.* **1952**, *37*, 950–959.
32. Deliens, M.; Piret, P. La rabejacite, $\text{Ca}(\text{UO}_2)_4(\text{SO}_4)_2(\text{OH})_6 \cdot 6\text{H}_2\text{O}$, nouveau sulfate d’uranyle et de calcium des gîtes du Lodévois, Hérault, France. *Eur. J. Mineral.* **1993**, *5*, 873–877. [[CrossRef](#)]
33. Meisser, N. *La Minéralogie de L’uranium dans le Massif des Aiguilles Rouges*; Matériaux pour la Géologie de la Suisse: Série Géotechnique; Office Fédéral de Topographie Swisstopo: Köniz, Switzerland, 2012; Volume 96, 183p.

34. Brugger, J.; Wallwork, K.S.; Meisser, N.; Ondruš, P.; Čejka, J. Pseudojohannite from Jáchymov, Musonoi and La Creusaz: A new member of the zippeite-group. *Am. Mineral.* **2006**, *91*, 929–936. [[CrossRef](#)]
35. Meisser, N.; Brugger, J.; Ansermet, S.; Thélin, P.; Bussy, F. Françoisite-(Ce), a new mineral species from La Creusaz uranium deposit (Valais, Switzerland) and from Radium Ridge (Flinders Ranges, South Australia): Description and genesis. *Am. Mineral.* **2010**, *95*, 1527–1532. [[CrossRef](#)]
36. Sheldrick, G.M. Crystal structure refinement with *SHELXL*. *Acta Crystallogr.* **2015**, *C71*, 3–8.
37. Burns, P.C.; Hawthorne, F.C.; Ewing, R.C. The crystal chemistry of hexavalent uranium: Polyhedron geometries, bond-valence parameters, and polymerization of polyhedra. *Can. Mineral.* **1997**, *35*, 1551–1570.
38. Gagné, O.C.; Hawthorne, F.C. Comprehensive derivation of bond-valence parameters for ion pairs involving oxygen. *Acta Crystallogr.* **2015**, *B71*, 562–578. [[CrossRef](#)]
39. Hawthorne, F.C.; Krivovichev, S.V.; Burns, P.C. The crystal chemistry of sulfate minerals. *Rev. Mineral. Geochem.* **2000**, *40*, 1–112. [[CrossRef](#)]
40. Krivovichev, S.V. Structural complexity of minerals: Information storage and processing in the mineral world. *Miner Mag.* **2013**, *77*, 275–326. [[CrossRef](#)]
41. Krivovichev, S.V. Which inorganic structures are the most complex? *Angew. Chem. Int. Ed.* **2014**, *53*, 654–661. [[CrossRef](#)]
42. Blatov, V.A.; Shevchenko, A.P.; Proserpio, D.M. Applied topological analysis of crystal structures with the program package ToposPro. *Cryst. Growth. Des.* **2014**, *14*, 3576–3586. [[CrossRef](#)]
43. Gurzhiy, V.V.; Plášil, J. Structural complexity of natural uranyl sulfates. *Acta Cryst. Sect. B* **2018**. accepted.
44. Gurzhiy, V.V.; Krivovichev, S.V.; Tananaev, I.G. Dehydration-driven evolution of topological complexity in ethylammonium uranyl selenates. *J. Solid State Chem.* **2017**, *247*, 105–112. [[CrossRef](#)]
45. Gurzhiy, V.V.; Tyumentseva, O.S.; Krivovichev, S.V.; Tananaev, I.G. Cyclic polyamines as templates for novel complex topologies in uranyl sulfates and selenates. *Z. Kristallogr.* **2018**, *233*, 233–245. [[CrossRef](#)]
46. Pankova, Y.A.; Gorelova, L.A.; Krivovichev, S.V.; Pekov, I.V. The crystal structure of ginorite, $\text{Ca}_2[\text{B}_{14}\text{O}_{20}(\text{OH})_6](\text{H}_2\text{O})_5$, and the analysis of dimensional reduction and structural complexity in the $\text{CaO-B}_2\text{O}_3\text{-H}_2\text{O}$ system. *Eur. J. Mineral.* **2018**, *30*, 277–287. [[CrossRef](#)]



© 2018 by the authors. Licensee MDPI, Basel, Switzerland. This article is an open access article distributed under the terms and conditions of the Creative Commons Attribution (CC BY) license (<http://creativecommons.org/licenses/by/4.0/>).